An Optimal Control Based Estimator for Maneuver and Natural Dynamics Reconstruction

Daniel P. Lubey and Daniel J. Scheeres
University of Colorado, Boulder, United States

ABSTRACT

With overcrowding threatening the safety of Earth's orbital environment, methods for tracking and understanding the motions of objects in orbit have become very important. This paper details an estimation algorithm that incorporates optimal control for the purposes of Maneuver Detection and Reconstruction. In this context, maneuver refers to any unmodeled acceleration: active spacecraft thrusting, unmodeled force, mismodeled force, etc. This estimation algorithm is composed of three components each of which is detailed in this paper. The first component is an estimator akin to a Kalman Algorithm, but with additional properties for more accurate tracking and reconstructing maneuvers through the generation of optimal control policies. The other two components are a maneuver detection algorithm that relies on measurement residuals, and a maneuver reconstruction algorithm that estimates mismodeled parameters for atmospheric drag and solar radiation pressure perturbations. The complete algorithm is demonstrated numerically in a simulation of a LEO spacecraft with mismodeled dynamics subject to independent tracking measurements.

1. INTRODUCTION

The Kalman Algorithm is a staple in the orbit determination community. It is easily implementable, and quite powerful when used properly. The basic algorithm has issues with divergence, saturation, maintaining a symmetric positive definite covariance matrix, and compensating for mismodeled dynamics, but these issues can generally be overcome by introducing a number of different complementary algorithms (e.g. inclusion of process noise, State Noise Compensation, Dynamic Model Compensation, Joseph Covariance Formulation, etc. [1]). These algorithms can be quite effective, but in certain cases they tend to neglect information. Specifically, the inclusion of process noise (State Noise Compensation - SNC) merely inflates the noise in the system so that the system can maintain tracking in the presence of small dynamic uncertainties. The algorithm neglects those underlying uncertainties, and provides no information on the mismodeled dynamics. In this paper we present a similar estimation algorithm that directly estimates the control (using a minimum fuel criterion), which may be used for maneuver detection, maneuver reconstruction, and natural dynamics estimation. This algorithm is paired with a post-processing algorithm that takes these control profiles and extracts natural dynamics information out of them.

The topics of Maneuver Detection and Reconstruction have been well-studied, but the resulting algorithms have generally been aimed at highly dynamical systems (such as missile tracking and guidance) and environments that are data-rich - neither of which can be used to describe orbital dynamics, generally. Methods such as Bar-Shalom and Birmiwal's Variable Dimension Filter [2] and Chan, Hu, and Plant's Input Estimation Method [3] directly append accelerations to the state vector for estimation when a maneuver is detected through residuals, but such methods require observation throughout a continuous maneuver. Patera's space event detection method [4] focuses more on quick events in an astrodynamics context, so it tends to neglect smaller maneuvers and natural dynamics mismodeling. Holzinger, Scheeres, and Alfriend [5] addressed the problems of object correlation, maneuver detection, and maneuver characterization for data sparse environments by implementing a Control Distance Metric based on a quadratic control policy. Singh, Horwood, and Poore [6] applied the Holzinger et al. results using a minimum-fuel cost function. Lubey and Scheeres [7] adapted these approaches to estimate mismodeled natural dynamics using optimal control policies (a modified version of this is developed into the post-processing natural dynamics estimation method presented in this paper). This paper uses this optimal control framework and adapts it into a filter formulation capable of state estimation, control estimation, maneuver detection, maneuver reconstruction, and natural dynamics estimation.

This study summarizes this estimation algorithm with development of the algorithm and numerical verification through simulations. Section II outlines all of the estimation algorithms developed in this paper including the Optimal

Control Estimator, Maneuver Detector, and the Natural Dynamics Estimator. Relevant background is also provided. In general, only final results are presented - references to papers with derivation are provided where appropriate. Section III presents some simulations in which these algorithms are implemented in a spacecraft tracking scenario. This is followed by a discussion of those results. Conclusions are given in Section IV with some suggestions for future work.

2. OPTIMAL CONTROL BASED ESTIMATION METHOD

In this section, the algorithms developed in this paper are defined and analyzed. Some background information in optimal control and distance metrics is provided to set a foundation. After establishing this foundation, the Optimal Control Estimator is described. Using the state estimates from this estimator we develop a maneuver detection algorithm, which relies on measurement residuals. Finally, an algorithm that analyzes the information content of the control profiles that come out of the Minimum Fuel Estimator is developed.

2.1. Optimal Control Policies and Distance Metrics

In this section the foundations of optimal control policies and distance metrics are explored in order to set a foundation for the algorithms developed in this paper. More detailed accounts are provided by Lawden [8,9], Marec [10], Stengel [11], and Prussing [12, 13] among others.

Optimal control policies are derived from a cost function as defined in Eqn. 1. In this notation the Lagrangian portion of the cost ($\mathcal{L}$) is evaluated across the entire time of flight, whereas the boundary costs (K_0 and K_f) are evaluated only at the initial and/or final epochs. In addition to these soft constraints, hard constraints are imposed via Lagrange multipliers ($\vec{\mu}_0$,$\vec{\mu}_f$, and $\vec{p}(t)$). The first two hard constraints force the initial and final times and states to lie on given manifolds ($g_0(\vec{x}_0, t_0) = \vec{0}$ and $g_f(\vec{x}_f, t_f) = \vec{0}$). The final hard constraint enforces the state dynamics to adhere to a given function of the state, control, and time ($\dot{\vec{x}}(t) = \vec{f}(\vec{x}(t), \vec{u}(t), t)$). The Lagrange multiplier that enforces this constraint ($\vec{p}(t)$) is termed the system's adjoint or costate.

$$\begin{aligned} J &= \left[K_0(\vec{x}_0, t_0) + \vec{\mu}_0^T g_0(\vec{x}_0, t_0)\right] + \left[K_f(\vec{x}_f, t_f) + \vec{\mu}_f^T g_f(\vec{x}_f, t_f)\right] \\ &\quad + \int_{t_0}^{t_f} \left[\mathcal{L}\left(\vec{x}(\tau), \vec{u}(\tau), \tau\right) + \vec{p}(\tau)^T \left(\vec{f}\left(\vec{x}(\tau), \vec{u}(\tau), \tau\right) - \dot{\vec{x}}(\tau)\right)\right] d\tau \end{aligned} \tag{1}$$

Minimizing (or maximizing) this cost function yields a set of necessary conditions. Generally one necessary condition relates the optimal control policy ($\vec{u}(t)$) to the state and adjoint. Two other necessary conditions define the state and adjoint dynamics. The final four necessary conditions, known as the transversality conditions, provide conditions on the boundary adjoints and times based on the boundary costs (both the soft and hard constraints). The control policy, dynamics, and transversality conditions are all used in the Optimal Control Estimator developed in this paper. The process may be rewritten as a Hamiltonian system, which provides useful properties of the solution. This includes a symplectic state transition matrix, which is used to manipulate the equations for the Optimal Control Estimator into a convenient form.

Beyond optimal control policies, control distance metrics also lie at the heart of algorithms developed in this study. The control distance metric was defined by Holzinger, Scheeres, and Alfriend [5], and also explored in Singh, Horwood, and Poore [6]. As defined in Eqn. 2, the distance metric defines the amount of control effort used to navigate from one state to another in a given amount of time using a single positive definite scalar quantity. A distance metric of zero implies that the states lie on a ballistic trajectory - this means that there are no unmodeled maneuvers or mismodeled dynamics on the arc.

$$d_C(a, b) = \int_{t_a}^{t_b} \frac{1}{2} \vec{u}(\tau)^T \vec{u}(\tau) d\tau \tag{2}$$

In reality, errors in the system will induce nonzero distance metrics even when dynamics are modeled perfectly. Chiefly, this occurs when there are errors in the boundary states due to imperfect tracking. In this case, a statistical approach must be taken. With the given amount of error in the system we can calculate an expected mean and spread for the distance metric, which allows us to define a threshold at which a statistically significant event occurs. This defines how this metric may be used for the purposes of maneuver detection.

Beyond just maneuver detection, we can characterize and reconstruct maneuvers using control distance metrics and optimal control policies. In this context maneuver refers to any type of unmodeled or mismodeled dynamics including

active thrusting by spacecraft or mismodeled natural dynamics. The distance metric itself provides a ΔV metric to characterize a maneuver. Beyond this we can use the optimal control policies to extract information about maneuvers. In Lubey and Scheeres [7] it was shown that optimal control policies derived from a quadratic control Lagrangian (as is used to define this control distance metric) mimic the natural dynamics they are replicating. Additionally, these control policies are also an upper-bound approximation for minimum fuel maneuvers (which we will assume all maneuvers are designed to be), so they represent unnatural thrusting patterns too. This assumption is based on the fact that fuel is an important non-renewable resource in orbit that must be conserved in order to prolong mission lifetime and maintain system capabilities.

An algorithm for tracking orbiting objects, detecting maneuvers by such objects, and reconstructing those maneuvers is describe in the following subsections. Each portion of the algorithm is discussed in a separate subsection.

2.2. Optimal Control Estimator

The derivation of the following estimator and maneuver detection algorithm can be found in Lubey and Scheeres [14]. Here, we present only the initial cost function terms and the final measurement update and control equations.

The Optimal Control Estimator, takes in measurements at given times and outputs a state estimate and associated control policy, from which additional information may be obtained. To understand how this estimator works it is necessary to understand the terms within the cost function that are used to derive it. Using a Bolza cost function of the form given in Eqn. 1 we define the associated Optimal Control Estimator costs in Eqn. 3. The cost function contains three different costs: (1) an initial soft constraint that attempts to select an initial state as close to the a priori information as possible (weighted by the a priori state information matrix), (2) a final soft constraint that attempts to select a final state as close the measurement manifold as possible (weighted by the data information matrix), and (3) a Lagrangian that limits the control magnitude throughout the measurement gap (weighted by a matrix that qualifies the system's dynamics uncertainty).

$$\begin{aligned} K_0(t_{k-1}, \vec{x}_{k-1}) &= \frac{1}{2} \left(\bar{x}_{k-1} - \vec{x}_{k-1}\right)^T \bar{P}_{k-1}^{-1} \left(\bar{x}_{k-1} - \vec{x}_{k-1}\right) \\ K_f(t_k, \vec{x}_k) &= \frac{1}{2} \left(\vec{Y}_k - h(t_k, \vec{x}_k)\right)^T R_k^{-1} \left(\vec{Y}_k - h(t_k, \vec{x}_k)\right) \\ \mathcal{L}\left(\vec{x}(t), \vec{u}(t), t\right) &= \frac{1}{2} \vec{u}(t)^T \tilde{Q}^{-1} \vec{u}(t) \end{aligned} \tag{3}$$

Unlike a typical Kalman Filter, the Minimum Fuel Estimator frees up the initial state and provides a control policy to the link the initial and final state estimates. By freeing up the initial condition, this estimator decouples the costs associated with a priori state uncertainty and dynamic uncertainty. In the Kalman algorithm these effects are coupled by ballistically propagating a priori information to the measurement epoch, and then assessing an a priori uncertainty cost. By decoupling these costs we can assess the contribution of each to the orbit determination process. Also, unlike the Kalman Filter, the Optimal Control Estimator has a dynamic uncertainty naturally included in it. Dynamic uncertainty greatly aids in tracking for systems with dynamic mismodeling, and it also prevents filter saturation. A Kalman Filter must be adapted to include dynamic uncertainty by including process noise through a SNC algorithm. Even with a SNC algorithm, the Kalman Algorithm does not provide any information on mismodeled dynamics, unlike the Optimal Control Estimator.

With a better understanding of how this estimator is formed and how it operates, we can begin to analyze its measurement update equations. To obtain the linear measurements update equations, we apply the transversality conditions to the boundary costs, then linearize about a ballistic nominal trajectory. Using the full state transition matrix definition of the system, we obtain four vector equations with four vector unknowns (initial and final states and adjoints). Applying ballistic and symplectic properties of the state transition matrix we can write the measurement update equations for this estimator as shown in Eqn. 4. The equations are written in Kalman-analagous formulation. In fact the only difference in the state equations is the a priori state covariance. This matrix is inflated with dynamic

uncertainty, meaning the estimator will favor measurement information over a ballistic propagation.

$$\begin{aligned} \delta\hat{x}_k &= \delta\bar{x}_k + L_k\left(\delta\vec{y}_k - \tilde{H}_k\delta\bar{x}_k\right) \\ L_k &= \mathcal{P}_k\tilde{H}_k^T\left(R_k + \tilde{H}_k\mathcal{P}_k\tilde{H}_k^T\right)^{-1} = \mathcal{P}_k\Psi_k \\ \mathcal{P}_k &= \bar{P}_k - \left(\Phi_{xp}\Phi_{xx}^T\right) \\ \hat{P}_k &= \left(I - L_k\tilde{H}_k\right)\mathcal{P}_k\left(I - L_k\tilde{H}_k\right)^T + L_kR_kL_k^T \end{aligned} \tag{4}$$

While the state equations are similar to a Kalman algorithm, the Optimal Control Estimator provides far more additional information through its control estimates. Along with state updates, the Minimum Fuel Estimator also has adjoint updates, through with the control is directly related as shown in Eqn. 5. Using these control profiles we can estimate mismodeled dynamics (active and natural) as described in the post-processing algorithm in the following subsections.

$$\begin{aligned} \delta\hat{p}_{k-1} &= -\Phi_{xx}^T\Psi_k\left(\delta\vec{y}_k - \tilde{H}_k\delta\bar{x}_k\right) \\ \vec{u}(t) &= -\tilde{Q}\frac{\partial\vec{f}\left(\vec{x}^*(t),\vec{u}^*(t),t\right)}{\partial\vec{u}}^T\Phi_{pp}(t,t_{k-1})\delta\hat{p}_{k-1} \end{aligned} \tag{5}$$

2.3. Maneuver Detection using Measurement Residuals

While, a nonzero control profile may be output by this estimator, it is possible that the control is symptomatic of the error in the system rather an actual unmodeled acceleration. Following a derivation by Holzinger, Scheeres, and Alfriend [5], we reformulate and adapt a control distance metric based maneuver detection algorithm to be implementable into the Minimum Fuel Estimator. Assuming the nominal trajectory is approximately truth (this works with an EKF implementation of the Minimum Fuel Estimator), we can write the control distance metric in terms of the prefit measurement residual as shown in Eqn. 6 with a definition in Eqn. 7.

$$P_C = \delta\vec{y}_k^T\left(\Psi_k^T\Phi_{xx}\Pi_k\Phi_{xx}^T\Psi_k\right)\delta\vec{y}_k \tag{6}$$

$$\Pi_k = \frac{1}{2}\int_{t_{k-1}}^{t_k}\Phi_{pp}(\tau,t_{k-1})^T\frac{\partial\vec{f}}{\partial\vec{u}}\tilde{Q}^T\tilde{Q}\frac{\partial\vec{f}}{\partial\vec{u}}^T\Phi_{pp}(\tau,t_{k-1})d\tau \tag{7}$$

As mentioned, a nonzero distance metric implies the states do not lie on a ballistic trajectory, which implies that either a maneuver occurred or error within the system generated the control policy. In order to determine whether the maneuver is genuine, we define a statistical threshold for the distance metric. A control distance metric beyond this threshold signals a maneuver. To define this threshold we approximate the distance metric as a Gaussian random variable that is influenced by two sources of error - the measurement error and the a priori state uncertainty. The mean and spread of this distribution are shown in Eqns. 8 and 9, respectively. In this study we generally use 95% confidence level to define the distance metric threshold.

$$\mu_P = Tr\left[\left(\Psi_k^T\Phi_{xx}\Pi_k\Phi_{xx}^T\Psi_k\right)R_k\right] + Tr\left[\left(\tilde{H}_k^T\Psi_k^T\Phi_{xx}\Pi_k\Phi_{xx}^T\Psi_k\tilde{H}_k\right)\bar{P}_k\right] \tag{8}$$

$$\begin{aligned} \sigma_P^2 &= 2Tr\left[\left(\Psi_k^T\Phi_{xx}\Pi_k\Phi_{xx}^T\Psi_kR_k\right)^2\right] + 2Tr\left[\left(\tilde{H}_k^T\Psi_k^T\Phi_{xx}\Pi_k\Phi_{xx}^T\Psi_k\tilde{H}_k\bar{P}_k\right)^2\right] \\ &\quad + 4Tr\left[\left(\tilde{H}_k^T\Psi_k^T\Phi_{xx}\Pi_k\Phi_{xx}^T\Psi_k\tilde{H}_k\right)\bar{P}_k\left(\Psi_k^T\Phi_{xx}\Pi_k\Phi_{xx}^T\Psi_k\right)R_k\right] \end{aligned} \tag{9}$$

Depending on where the threshold is defined, false positives may be thrown or smaller maneuvers may be neglected. For constant biases (such as mismodeled drag), though, we find that maneuvers are detected consistently until the dynamic uncertainty level is adjusted to match the true uncertainty. Once a maneuver is detected we initiate a process of characterizing and reconstructing the maneuver. The distance metric itself characterizes the maneuver, when mapped into ΔV space [5]. Reconstruction is accomplished by analyzing the estimated control profile. One such method for this analysis is documented in the following subsection.

2.4. Post-Processing Control Profile Analysis

The following control profile analysis is adapted from Lubey and Scheeres [7]. In this algorithm, we take control profiles in which maneuvers have been detected, and extract information about mismodeled natural dynamics. We specifically focus on modeling atmospheric drag and solar radiation pressure since these perturbations are object dependent (unlike gravitational perturbations), thus are most likely to contain the largest amounts of error. This process is accomplished by minimizing distance metric-like cost function that attributes control accelerations to drag and SRP accelerations. The algorithm outputs improved estimates for the drag and SRP parameters that may be used to update the dynamical model.

The algorithm assumes that natural dynamics may be adequately replicated by an optimal control policy. This was demonstrated for drag and SRP with quadratic optimal control policies in Lubey and Scheeres [7]. These results are summarized in Fig. 1. In this example both drag and SRP are mismodeled for a LEO spacecraft, and Optimal Control Policy (OCP) is generated to replicate the missing dynamics (i.e. the mismodeled natural dynamics). These results show that the two acceleration profiles remain aligned with one another (to within 0.3 degrees), and the magnitudes are incredibly close with the same periodicity. This demonstrates that OCPs are a good approximation for mismodeled drag and SRP accelerations.

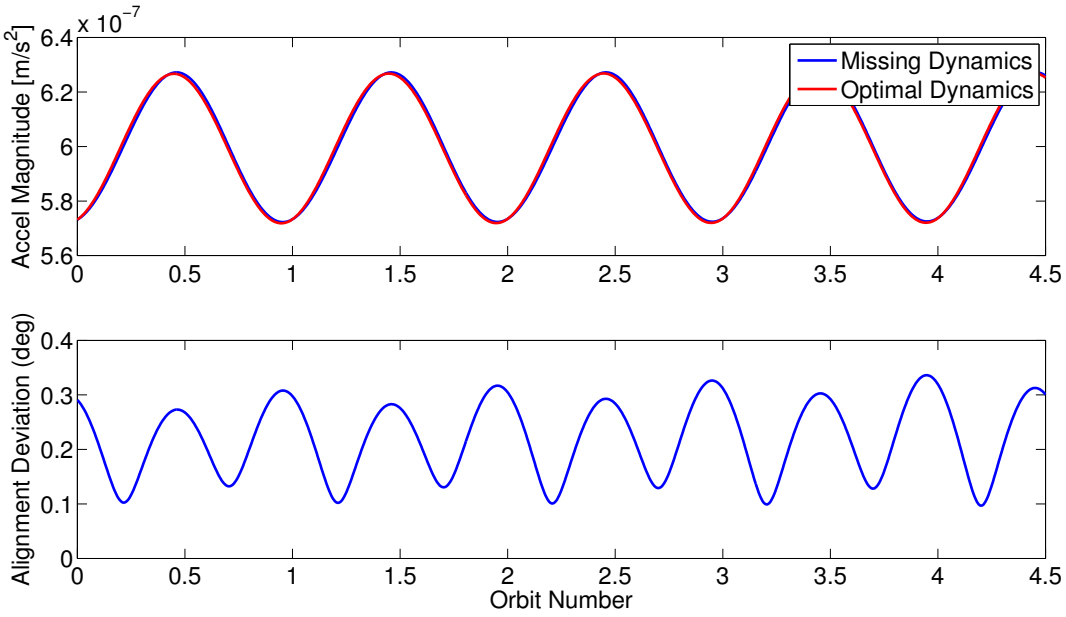

Figure 1: Optimal Control Policy with Mismodeled Atmospheric Drag and SRP. (Top) Missing and OCP Magnitude. (Bottom) Alignment of OCP with Missing Dynamics

To extract information from these control policies we employ the estimation algorithm defined by Eqns. 10 - 13. In these equations, $\Delta\vec{C}$ represents the change from nominal in the drag and SRP parameters, $P_{\Delta C}$ represents the expected uncertainty in the drag and SRP parameters, $\delta\vec{z}$ represents the deviation from the given boundary states, and P_Z represents the uncertainty in the boundary states.

$$\begin{aligned}\Delta\vec{C} \;=\; & \left(\int_{t_a}^{t_b} A(\vec{x}^*(\tau),\tau)^T A(\vec{x}^*(\tau),\tau)d\tau\right)^{-1}\left[\int_{t_a}^{t_b} A(\vec{x}^*(\tau),\tau)^T\vec{u}^*(\tau)d\tau\right. \\ & \left.-\left(\int_{t_a}^{t_b} A(\vec{x}^*(\tau),\tau)^T\tilde{Q}\frac{\partial\vec{f}}{\partial\vec{u}}^T\Lambda(t,t_0)d\tau\right)\delta\vec{z}\right]\end{aligned} \tag{10}$$

$$P_{\Delta C} = \left(\int_{t_a}^{t_b} A(\vec{x}^*(\tau),\tau)^T A(\vec{x}^*(\tau),\tau)d\tau\right)^{-1} \left(\int_{t_a}^{t_b} A(\vec{x}^*(\tau),\tau)^T \tilde{Q} \frac{\partial \vec{f}}{\partial \vec{u}}^T \Lambda(t,t_0)d\tau\right) P_z \tag{11}$$
$$\times \left(\int_{t_a}^{t_b} \Lambda(t,t_0)^T \frac{\partial \vec{f}}{\partial \vec{u}} \tilde{Q}^T A(\vec{x}^*(\tau),\tau)d\tau\right) \left(\int_{t_a}^{t_b} A(\vec{x}^*(\tau),\tau)^T A(\vec{x}^*(\tau),\tau)d\tau\right)^{-1}$$

$$A(\vec{x}(t),t) = \left[\ \tilde{a}_{Drag}(t,\vec{x}(t)) \quad \tilde{a}_{SRP}(t,\vec{x}(t))\ \right] \tag{12}$$

$$\Lambda(t,t_0) = \left[\ \Phi_{px}(t,t_0) - \Phi_{pp}(t,t_0)\Phi_{xp}(t_f,t_0)^\dagger \Phi_{xx}(t_f,t_0) \quad \Phi_{pp}(t,t_0)\Phi_{xp}(t_f,t_0)^\dagger\ \right] \tag{13}$$

In general, if maneuver detection indicates a consistent bias this analysis should be employed to determine is drag and SRP mismodeling are to blame. Estimates may be obtained for each new measurement, and all those estimates may be combined in a Least Squares method to form a single dynamics parameter estimate with an associated uncertainty. Based on the application, this process may be repeated by updating the dynamical model with the new estimates, then running the measurements through the estimator again. Successive iterations drive this method closer and closer to truth as is shown in the simulation in the following section.

3. SIMULATIONS AND RESULTS

To demonstrate the capabilities of this algorithm, we provide a numerical simulation in which a LEO spacecraft is tracked for 150 hours via range and range-rate measurements. Measurements are taken once every hour from one of three GEO spacecraft depending on which one has the best view of the spacecraft. White Gaussian noise of 0.1 m and 1 mm/s is added to the measurements. Initial conditions and true dynamics parameters for this simulation are given in Table 1.

Table 1: True Spacecraft Parameters and Initial Conditions for Test Case

Parameter	Symbol	Value	Units
Mass	m	970	kg
Drag Parameter	B	0.0062	m^2/kg
SRP Parameter	P	0.0031	m^2/kg
Initial Semimajor Axis	a_0	7172.498	km
Initial Eccentricity	e_0	0.001	-
Initial Inclination	i_0	98.620	deg
Initial Right Asc. of the Asc. Node	Ω_0	253.734	deg
Initial Argument of Perigee	ω_0	77.203	deg
Initial Mean Anomaly	M_0	59.490	deg

To initially test this algorithm we track the spacecraft with an incorrect dynamical model. In this case we have 12.5% overestimate in the drag parameter, so there tends to be a consistent bias in the along-track acceleration with a small radial direction coupling due to the eccentricity of the orbit. Maneuvers are defined using a 95% threshold as discussed previously. To demonstrate the effect dynamic noise has tracking performance we run the estimator at various level of dynamic error, and also perform maneuver detection calculations.

The tracking performance as a function of dynamic uncertainty is summarized in Fig. 2. In these results we see that tracking is best for dynamic uncertainties of 1E-08 m/s^2, which makes sense because with this level of drag mismodeling there are uncertainties in the acceleration on the order of 1E-08 m/s^2. This is further confirmed by the maneuver detection results as shown in Fig. 3. In these results, any value above 1 indicates maneuver was detected since the results are a fraction with respect to the threshold distance metric level. For lower levels of dynamic uncertainty maneuvers are detected on a consistent basis because the dynamic uncertainty does not represent the true error in the system. As we converge on the appropriate level of uncertainty, maneuvers are not detected as frequently. Only a few points out the 150 points eclipse the threshold, which is to be expected since a 95% level was chosen as the threshold. In this manner, the maneuver detection results may be used to tune the dynamic uncertainty level so that biases are ignored - those biases can then be addressed by the controls analysis algorithm. To make a special note, the tracking results indicate that the Kalman Algorithm without process noise and the zero dynamic uncertainty case are

identical. This property (also verifiable analytically) demonstrates the connection this algorithm has with a Kalman Filter.

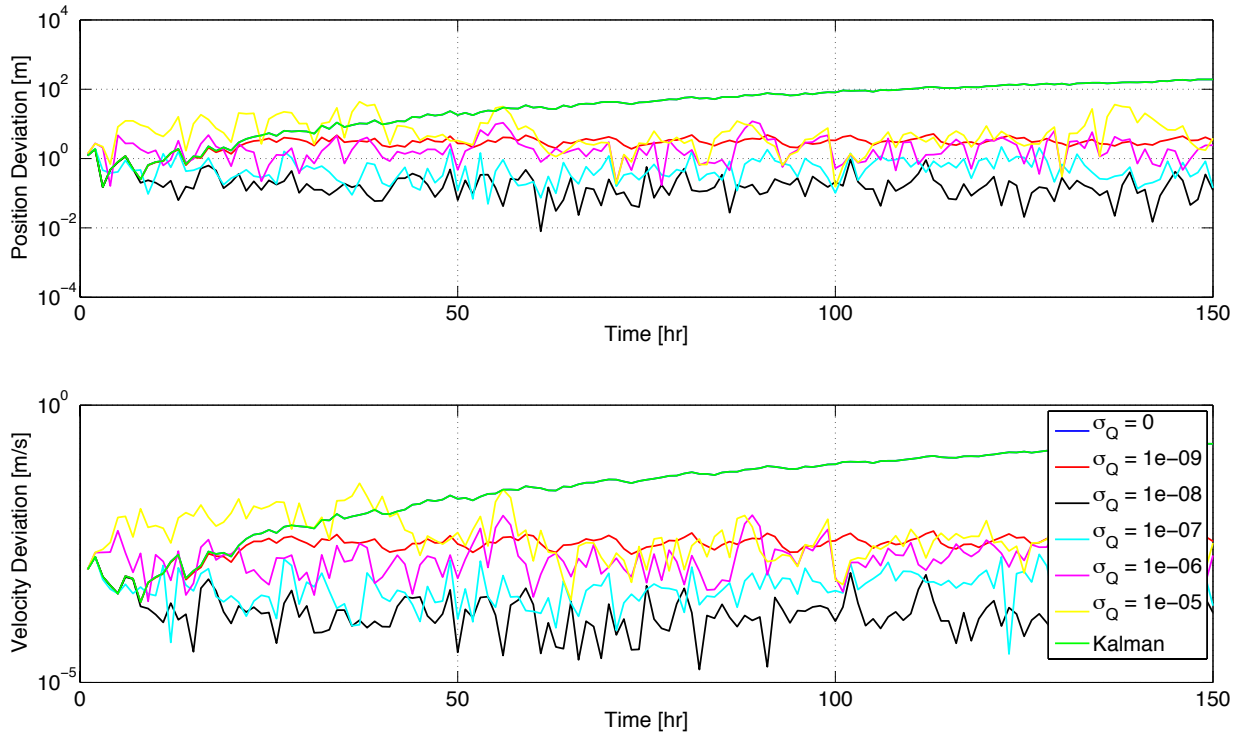

Figure 2: State estimate deviations from truth. Position (top) and velocity (Bottom). σ_Q is the level of uncertainty in the dynamics in m/s^2.

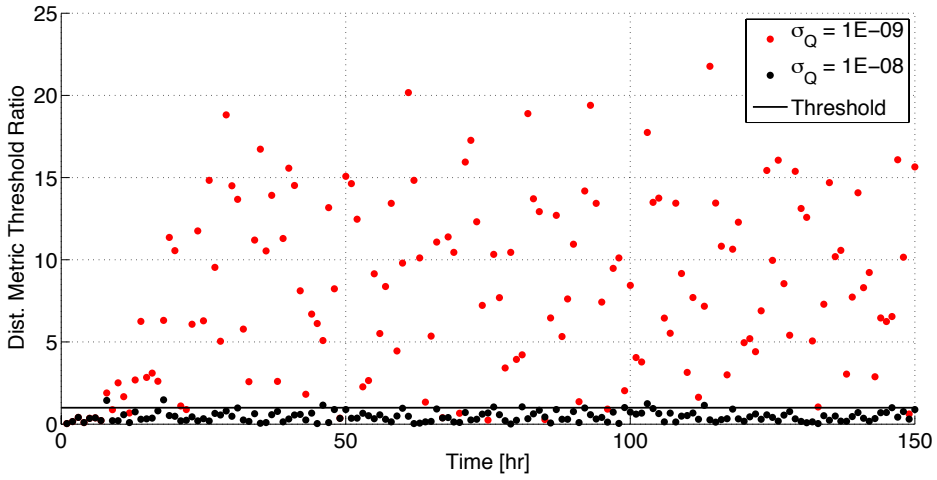

Figure 3: Maneuver detection results for dynamic uncertainty levels of σ_Q = 1e-09 (red) and 1e-08 (black) m/s^2.

Once settled on a level of dynamic uncertainty, we can filter all of the measurements and calculate state estimates with associated control profiles. The control profiles are shown in Fig. 4. The control is subject to noise, so we do not clearly see a consistent bias in control, but it can be seen that the radial and along track control are not centered on zero. Both shifted slightly upward and tend to favor non-negative control, which is indicative of a biased acceleration in these directions (with along - track being the stronger bias).

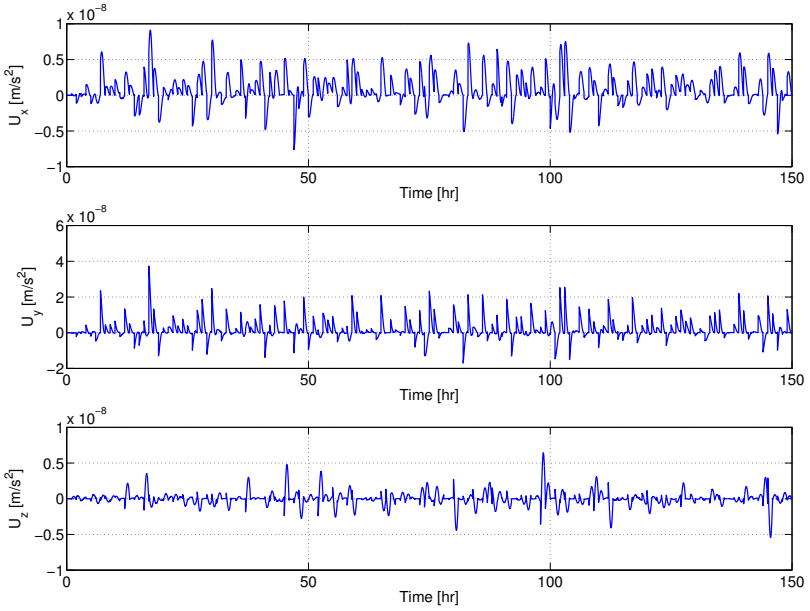

Figure 4: Estimated control profiles in Hill frame (radial, along track, cross track) for mismodeled drag example.

The bias is identifiable in the control policies. This is confirmed by the post-processing controls analysis algorithm. All of these control policies yield an estimate for both the drag and SRP parameters. The results of this post-processing estimation is shown in Fig. 5. In this plot, the blue dots represent the individual 150 parameter estimates, the black dot represents the modeled values, the red represents the true values, and the magenta dot represents the final estimate once all the individual estimates are combined in a least squares calculation. These results show that the bias is identified in this algorithm, and the updated estimate brings the system's dynamics closer to truth. If we iterate the process, we can drive the system even closer to truth.

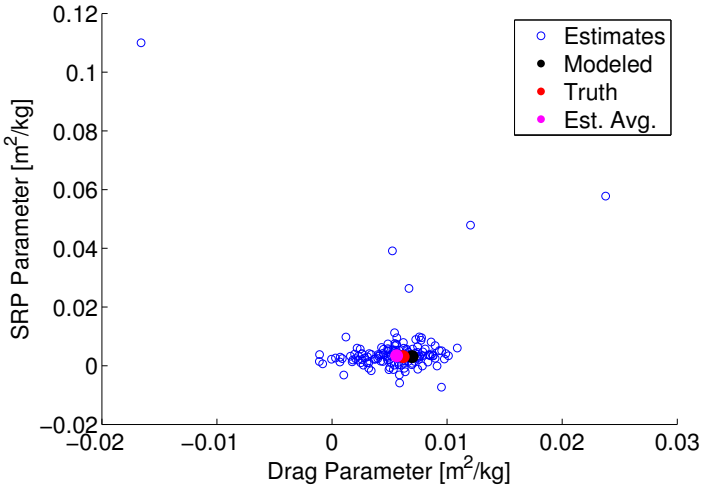

Figure 5: Estimated dynamics parameters calculated from control profiles.

To iterate this process, the measurements are filtered, then the controls are analyzed to produce a new estimate of the dynamics parameters. With these estimated parameters, the dynamical model is updated, and the measurements

are refiltered. This may be repeated as often as desired, until the process converged on a parameter set. Results from iterated estimation are given in Table 2. These results specifically focus on drag estimation, because for a LEO spacecraft drag is orders of magnitude stronger than SRP. This can cause issues with SRP estimation, so this capability is switched off for low altitude applications (similarly SRP is the focus for high altitude estimation).

These results show that the algorithm generally converges on truth. Subsequent iterations will tend to maintain error on the order of 0.1% though because, this is the limit of the information within the system. This makes sense because the covariance on the drag parameter puts the one sigma level at 0.3% of the true parameter. As such, estimates will dance around truth once reaching this level of accuracy.

Table 2: Drag estimates from controls analysis algorithm.

Iteration	Drag Estimate (m^2/kg)	Percent Error (%)
0	0.006959	12.50%
1	0.005608	9.33%
2	0.006443	4.16%
3	0.006056	2.10%
4	0.006256	1.15%
5	0.006125	0.98%

4. CONCLUSIONS AND FUTURE WORK

In this paper, we developed a complete algorithm for tracking an object in orbit, determining if that object is maneuvering (has unmodeled or mismodeled accelerations), and reconstructing those maneuvers. The algorithm takes the form of a typical estimator with a Kalman-like formulation, which allows for direct comparison. Unlike the Kalman algorithm, this estimator automatically includes dynamic uncertainty in its algorithm, it decouples the effects of a priori state uncertainty and dynamic uncertainty, it frees up the initial state, and it provides estimates of maneuvers through estimated optimal control profiles. So, while the estimator resembles a Kalman algorithm it actually is unique with its own useful tracking properties.

The maneuver detection and reconstruction algorithms rely only on the measurement residuals from the estimation algorithm and the control policies, so all three algorithms may be easily integrated together.

A simulation in which drag is mismodeled for a LEO spacecraft demonstrates how these algorithms may be implemented for a real-life tracking application. The results showed that the level of dynamic uncertainty is easily detectable, and the biasing due to drag mismodeling is clear in both the control policies and the analysis of these control policies. We demonstrated the effectiveness of all three algorithms by maintaining tight tracking of the spacecraft even with a flawed dynamical model, correctly identifying biasing with the maneuver detection algorithm, and accurately estimating the true drag parameter of the spacecraft using the control policies analysis algorithm.

In terms of future work, we seek to further adapt this algorithm for application in tracking problems. The algorithm should be made as automatic as possible, and it should uniquely estimate maneuvers and natural dynamics mismodeling for data-sparse applications.

ACKNOWLEDGEMENTS

This work was supported by a NASA Office of the Chief Technologists Space Technology Research Fellowship.

References

[1] Tapley, B.D., Schutz, B.E., & Born G.H., *Statistical Orbit Determination*, Elsevier Academic Press, 2004.

[2] Bar-Shalom, Y. & Birmiwal, K., *Variable Dimension Filter for Maneuvering Target Tracking*, Aerospace and Electronic Systems, Vol. 18, No. 5, pp. 621-629, 1982.

[3] Chan, Y.T., Hu, A.G.C., & Plant, J.B., *A Kalman Filter Based Tracking Scheme with Input Estimation*, Aerospace and Electronic Systems, Vol. 15, No. 2, pp. 237-244, 1979.

[4] Patera, R.P., *Space Event Detection Method*, Journal of Spacecraft and Rockets, Vol. 45, No. 3, 2008.

[5] Holzinger, M.J., Scheeres, D.J., & Alfriend, K.T., *Object correlation, maneuver detection, and characterization using control distance metrics*, Journal of Guidance, Control, and Dynamics, In Press 2011.

[6] Singh N., Horwood J.T., & Poore A.B., *Space Object Maneuver Detection Via a Joint Optimal Control and Multiple Hypothesis Tracking Approach*, AAS 12-159, In Press 2012.

[7] Lubey, D.P. & Scheeres, D.J., *Identifying and Quantifying Mismodeled Dynamics via Optimal Control Problem Distance Metrics*, Proceedings of the 2012 AIAA/AAS Astrodynamics Specialists Meeting, August 2012.

[8] Lawden, D.F., *Optimal Trajectories for Space Navigation*, Butterworths Mathematical Texts, 1963.

[9] Lawden, D.F., *Analytical Methods of Optimization*, Dover Publications Inc., 1975.

[10] Marec, J.P., *Optimal Space Trajectories*, Elsevier Press, 1979.

[11] Stengel, R.F., *Optimal Control and Estimation*, Dover Publications Inc., 1986.

[12] Prussing, J.E. & Chiu, J.H., *Optimal Multiple-Impulse Time-Fixed Rendezvous Between Circular Orbits*, AIAA Journal, Vol. 9, No.1, Feb. 1986.

[13] Prussing, J.E., *Optimal Two- and Three-Impulse Fixed-Time Rendezvous in the Vicinity of a Circular Orbit*, AIAA Journal, Vol. 8, No. 7, 1970, pp. 1221-1228.

[14] Lubey, D.P. & Scheeres, D.J., *An Optimal Control Based Estimator for Maneuver Detection and Reconstruction*, Proceedings of the 2013 AAS/AIAA Astrodynamics Specialists Meeting, August 2013.